Theor Chem Acc (2011) 130:299–304
DOI 10.1007/s00214-011-0976-y

REGULAR ARTICLE

Solvent effect on (2,2,6,6-Tetramethylpiperidine-1-yl)oxyl (TEMPO): a RISM-SCF-SEDD study

Marvin Jose F. Fernandez · Hirofumi Sato

Received: 11 March 2011 / Accepted: 9 June 2011 / Published online: 24 June 2011

Abstract The solvent dependence of several properties of (2,2,6,6-Tetramethylpiperidine-1-yl)oxyl (TEMPO) is investigated by the reference interaction site model self-consistent field (RISM-SCF) theory. Time-dependent density functional theory (TDDFT) coupled with RISM-SCF-SEDD (spatial electron density distribution) is used to evaluate the $n \rightarrow \pi^*$ transition energies and the results are compared to the reported experimental values.

Keywords TEMPO · RISM-SCF-SEDD · Solvatochromism · Absorption · TDDFT

1 Introduction

Radicals, both fleeting intermediates and stable compounds, have generated much current research interest [1]. Persistent nitroxide radicals are of particular significance because of their wide applicability in radical polymerization [2–4] and photochemical reactions [5, 6]. These radicals play an important role in biological systems as antioxidants, spin traps, spin labels and in magnetic resonance imaging applications and materials chemistry [7–9]. Interestingly, these radicals generally possess very low toxicity and are not mutagenic [10].

One of the more widely used nitroxyl radicals is (2,2,6,6-Tetramethylpiperidine-1-yl)oxyl (TEMPO) [11], a stable free radical compound first prepared by Lebelev and Kazarnovskii in 1960 [12]. TEMPO was the first nonconjugated nitroxyl radical to be synthesized and its persistent free radical nature has been attributed to the kinetic stability imparted by the presence of its bulky substituents [13]. The steric crowding around the radical center makes it physically difficult for the radical to react with another molecule [14]. Stable nitroxide radicals such as TEMPO are also well-known quenchers of excited singlet, doublet, and triplet states [15].

TEMPO is widely used in the oxidation of several functional groups [16, 17], particularly on its application in the oxidation of primary and secondary alcohols [18]. The excellent solubility of TEMPO in both polar and nonpolar organic solvents and water has also lead to its use as a standard base for the measurements of Lewis acidity of solvents by monitoring $n \rightarrow \pi^*$ transition [19]. An earlier study [20] reported the TEMPO solvatochromism and electronic distribution through the time-dependent density functional theory (TDDFT) frame with the polarizable continuum model (PCM) solvation.

In this work, we investigate the solvent dependence of several properties of TEMPO using the reference interaction site model self-consistent field [21–24] with spatial electron density distribution (RISM-SCF-SEDD) [25, 26], an ab initio electronic structure theory that takes account of the solvent reaction field in molecular detail. This theory simultaneously optimizes the electronic structure of the solute in solution and the statistical distribution of the solvent molecules around it. In recent work, the method was applied to excitation energy of aqueous solvation of

Dedicated to Professor Shigeru Nagase on the occasion of his 65th birthday and published as part of the Nagase Festschrift Issue.

M. J. F. Fernandez
Department of Chemistry, MSU-Iligan Institute of Technology, Iligan City 9200, Philippines

H. Sato (✉)
Department of Molecular Engineering, Kyoto University, Kyoto 615-8510, Japan
e-mail: hirofumi@moleng.kyoto-u.ac.jp

p-aminobenzonitrile over a wide range of thermodynamic conditions based on CASSCF and MCQDPT2 methods [27]. TDDFT coupled with RISM-SCF-SEDD is used here to evaluate the $n \rightarrow \pi^*$ transition energies and the calculated results are compared to the reported experimental values.

2 Computational details

Geometry optimizations and frequency calculations, in vacuo and in solution, basically employed BPW91 [29, 30] method based on the unrestricted treatment with the 6-31G(d) basis set. The effects from diffuse basis set, the functional in DFT, and the long-range (LC) correction were also checked. The electronic structure of TEMPO in solution and the distribution of the solvent around it were solved in a self-consistent manner by RISM-SCF-SEDD [25, 26]. It combines *ab initio* electronic structure theory and statistical mechanical theory of molecular liquid. Total energy of solvation system is defined as the sum of quantum chemical energy of the solute (E_{solute}) and solvation free energy ($\Delta\mu$) [24].

$$\mathscr{A} = E_{\text{solute}} + \Delta\mu = \langle\Psi|H_0|\Psi\rangle + \Delta\mu. \tag{1}$$

Since the electronic structure of the solute molecule and the solvation structure around it are determined in a self-consistent manner, the wave function of the solute molecule is distorted from that in the isolated state. Solvation free energy in the present framework of the theory (excess chemical potential derived under the hypernetted chain (HNC) approximation) is given by

$$\Delta\mu = -\frac{\rho}{\beta}\sum_{\alpha s}\int d\mathbf{r}\left[c_{\alpha s}(r) - \frac{1}{2}h_{\alpha s}^2(r) + \frac{1}{2}h_{\alpha s}(r)c_{\alpha s}(r)\right], \tag{2}$$

where $h_{\alpha\ s}(r)$ and $c_{\alpha\ s}(r)$ are respectively total and direct correlation functions between solute site α and solvent site s. $\beta = 1/k_{\text{B}}T$, where k_{B} and T are the Boltzmann constant and temperature, ρ is number density of solvent. Applying variational principle to Eq. (1), the Fock operator of the RISM-SCF theory (F^{solv}) including a solute-solvent interaction is naturally derived [24].

It is well established that the N–O group is responsible for the absorption, and n, π and π^* orbitals are generated from the combination of the nitrogen and oxygen orbitals. Both of n and π orbitals are doubly occupied and π^* is singly occupied in the ground state of doublet state [20]. Excitation energies corresponding to the $n \rightarrow \pi^*$ transition were investigated by TDDFT calculations coupled with RISM-SCF-SEDD method. Molecular orbital calculations were performed with the GAMESS [28] package modified by us.

The RISM equations were solved with HNC approximation [31] at $T = 298.15$ K. All the Lennard-Jones parameters used in this work are summarized in Table 1. The parameters employed for the atoms in the solute molecule were taken from the OPLS parameter set [32]. To describe the water solvent, the SPC-like water model [23] was used. Methanol [33, 34], acetonitrile [35], and dichloromethane [36] were also used as solvents.

Table 1 Parameters used for the computations

atom	σ/Å	ε/kcal mol^{-1}	q/|e|
TEMPO			
C	3.750	0.110	–[a]
H	1.000	0.056	–[a]
N	3.250	0.170	–[a]
O	3.166	0.155	–[a]
Solvent H_2O ($\rho = 1.00$ g/cm^3)			
O	3.166	0.155	−0.820
H	1.000	0.056	0.410
Solvent CH_3OH ($\rho = 0.79$g/cm^3)			
CH_3	3.775	0.207	0.265
O	3.070	0.170	−0.700
H	1.000	0.056	0.435
Solvent CH_3CN ($\rho = 0.81$g/cm^3)			
CH_3	3.775	0.207	0.150
C	3.650	0.150	0.280
N	3.200	0.170	−0.430
Solvent CH_2Cl_2 ($\rho = 1.32$g/cm^3)			
C	3.400	0.109	−0.363
Cl	3.471	0.265	−0.037
H	2.293	0.016	0.218

[a] Determined by RISM-SCF-SEDD procedure. See the text for the details

3 Results and discussion

3.1 Optimized geometry

The optimized geometry of TEMPO is shown in Fig. 1 and the pertinent structural parameters are given in Table 2. As is well known, the ring elaborates chair conformation with C_s symmetry, in which O1, N1, C1, and two hydrogen atoms lie in the symmetry plane. The calculations give good agreement to experimental X-ray diffraction data [37, 38], although the bond lengths of N–O and C3–N are slightly overestimated. The geometry in aqueous solution is not significantly different from the gas phase one: The lengths of the C-C bonds are negligibly decreased (by about 0.002–0.004 Å) as well as the C–N bond (0.001 Å). On the contrary, the N–O bond length is slightly increased (+0.004 Å). As discussed later, this should be related to the specific solvation on the oxygen atom that is exposed to the

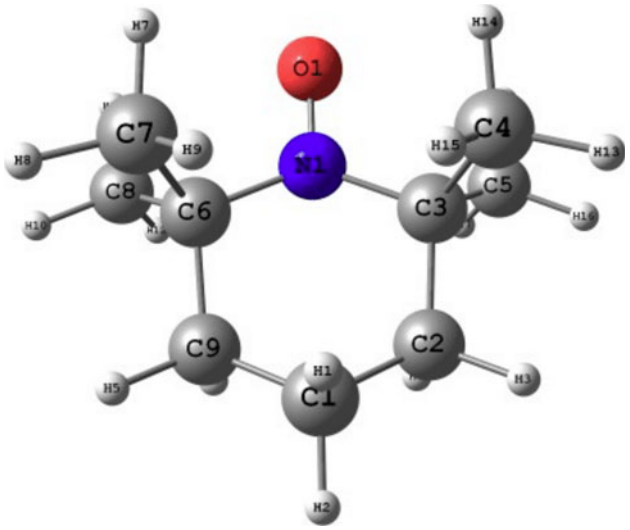

Fig. 1 2,2,6,6-Tetramethylpiperidine-1-oxyl (TEMPO) and the atom labels

Table 2 Selected optimized structural parameters of TEMPO compared to reported X-ray diffraction data

	Vacuum[a]	Aqueous	Expt [35, 36]
Bond length/Å			
N–O	1.292	1.296	1.283
C1–C2	1.533	1.530	1.508
C2–C3	1.547	1.543	1.520
C3–C4	1.548	1.544	1.543
C3–C5	1.542	1.539	1.513
C3–N	1.510	1.511	1.488
Bond angles/deg.			
C3–N–O	115.7	115.8	116.7
C3–(NO)–C6	124.4	124.7	123.6
C1–C2–C3	113.6	113.6	113.5
C2–C3–N	110.3	109.9	110.6

[a] Total Energy = −483.63953 a.u

solvent area. The weakening of double-bond character of N–O strengthens N–C and other C–C bonds. Anyway, the structural parameters calculated in the presence of water solvent have very minimal variation when compared to the values computed in vacuo. For this work, the general agreement between the calculated and experimental structural parameters should be sufficient to analyze trends in the solvation dependence of TEMPO's properties. Thus, to reduce the computational load, the gas-phase optimized geometry is used in the subsequent computations to assess the effects of various solvents.

3.2 Absorption energy

The pertinent data are shown in Table 3. The computed values show reasonable agreement with the corresponding

Table 3 Excitation energy, orbital energies, and their gap (eV)

	Excitation energy/eV		$\Delta\varepsilon^{b}$	ε^{β}_{43}	ε^{β}_{44}
	Calc	Expt[a]			
Vacuum	2.647	—	2.767	-4.898	−2.131
CH_2Cl_2	2.694	2.688	2.781	−5.366	−2.585
CH_3CN	2.706	2.688	2.792	−4.838	−2.046
CH_3OH	2.744	2.778	2.825	−5.437	−2.612
H_2O	2.773	2.921	2.846	−6.109	−3.263

[a] Ref. [19]. [b] $\Delta\varepsilon = \varepsilon^{\beta}_{44} - \varepsilon^{\beta}_{43}$, where ε^{β}_{43} and ε^{β}_{44} are HDOMO and SOMO in β electron orbital, respectively

experiments though all of them slightly underestimate. A clear trend is seen, namely, the excitation energy is systematically blue-shifted with increasing polarity of solvent. As for the choice of basis set, no evaluation was done as previous TDDFT studies [20, 39] have reported that the use of extended basis set or the use of a triple-ζ basis set do not lead to significant changes in excitation energies. In fact, by adding diffuse function on oxygen ($\alpha_{s/p} = 0.0845$) and nitrogen ($\alpha_{s/p} = 0.0639$), the evaluated energy in vacuo was 2.633 eV. We then examined other functionals, e.g., B3LYP, PW91, BPW91, PBE, and PBE0, but results from these calculations indicate that the choice of the functional has minimal influence on the calculated excitation energies, with a difference of only 0.0371 eV between the highest and lowest calculated values for the first excited state. Furthermore, BLYP with LC correction gave 2.597 eV, indicating that these contributions do not improve the quantitative agreement with experimental value. The present computational results are close to the PCM computations [20]. While the excitation energies in acetonitrile and in methanol slightly lower than those (2.75 and 2.77 eV, respectively), that in aqueous solution is almost the same although the hydrogen-bonding effect is taken into account in the present study. They reported that the excitation energy was overestimated with explicit water molecule. It should be noted that, as differentiated from the dielectric continuum model, the present RISM-SCF-SEDD method directly treats specific solvation at the molecular level. At all events, we would like to emphasize that the trend of the solvation effect is adequately described with the present theory. It is noted that the reported value in Ref. [19] is the absorption maximum of spectrum that is generally broad in solution phase. The computed value listed above corresponds to thermally averaged excitation energy, which is not necessary to be coincided with the absorption maximum because several sources are conceivable to broaden (and/or shift) the spectra in solution phase.

TDDFT computations clearly indicate that the absorption is attributed to HDOMO (the highest doubly occupied molecular orbital) → SOMO in β electron, both of them

Table 4 Dipole moment (μ), Mulliken charge on oxygen and nitrogen (q), and atomic spin density (SD)

	μ/D	q_N/|e|	q_O/|e|	SD_N/a.u.	SD_O/a.u.
Vacuum	2.83	−0.017	−0.384	0.1057	0.0485
CH_2Cl_2	3.27	−0.016	−0.399	0.1071	0.0479
CH_3CN	3.67	−0.014	−0.408	0.1082	0.0475
CH_3OH	4.10	−0.012	−0.438	0.1115	0.0461
H_2O	4.65	−0.013	−0.463	0.1139	0.0448

localized in N–O group. The former, HDOMO, is *n* orbital mainly located at the oxygen atom while the latter is π^* orbital on the oxygen-nitrogen atoms. The orbital gap between them shows good correlation with the TDDFT results as shown in Table 3. Hence, there are two types of overlap between the orbitals of nitrogen and oxygen that make the bond order of the N–O atom pair almost 2, namely σ-bond and π-bond. But π^* orbital is occupied by α electron and the presence of this unpaired electron on the anti-bonding π^* orbital partly counteracts the bonding π orbital, slightly decreasing the π bond character. Bond order analysis of the N–O atom pair shows it has a bond order of 1.393 (vacuo), larger than a single bond but not quite a double bond. The character of the bond is affected by solvation, and the order is decreased as increasing the polarity of solvent, namely 1.390 (CH_2Cl_2), 1.389 (CH_3CN), 1.383 (CH_3OH), and 1.375 (H_2O). The energy shift of each orbital caused by solvation effect may not look simple at first glance but should be systematically understood [40].

Table 4 summarizes the solvent effects on the computed dipole moment, Mulliken charge, and atomic spin density of TEMPO. The oxygen is the most affected by the presence of water solvent and its Mulliken charge becomes slightly more negative on going from the gas phase into solution. The charges on N and the two α–C's (C3 and C8) are relatively unaffected by the presence of solvent but the charges on all the other C atoms are made slightly negative (not shown). The dipole moment is clearly enhanced on going from the gas phase to the aqueous solution. The largest contribution of the spin density is found at nitrogen atom whose charge is nearly zero.

3.3 Solvation properties

In RISM-SCF combined with HNC closure, solvation free energy $\Delta\mu$ is analytically given by Eq. (2). Since the expression is "formally" a sum of the solute-solvent site-site interactions, the contribution of a specific atom α to the solvation free energy is defined. As shown in Table 5, the greatest single contribution to the negative free energy comes from the oxygen of TEMPO in methanol and

Table 5 Solvation free energy components of oxygen and nitrogen (kcal mol^{-1})

Group	CH_2Cl_2	CH_3CN	CH_3OH	H_2O
N	0.10	0.94	0.95	3.23
O	19.90	2.69	−3.51	−9.08

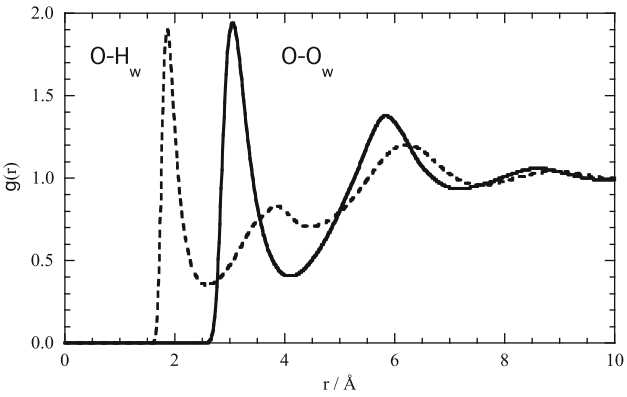

Fig. 2 Pair correlation function between the oxygen in TEMPO and the solvent water molecules. The *continuous lines* represent the interaction of the solute with the solvent oxygen while the *broken lines* are that of the solute with the solvent hydrogen

aqueous solution. This observation, however, is not applicable to the dichloromethane and acetonitrile solutions. On the other hand, the contribution from nitrogen is generally small for all solvents considered in this study.

To explore the solvation effects of water in more detail, the site-site pair correlation functions (PCF) for all the combinations of atom pairs between TEMPO and the solvent water molecules are examined. Shown in Fig. 2 is the PCF between the oxygen of the solute and the atoms of the solvent. The sharp peak around 1.9 Å is an evidence of the strong hydrogen bond between the oxygen of the solute and the hydrogen in the solvent. The higher peak around 3.0 Å is the O–Ow (solvent water oxygen) interaction between the solute and the solvent. It is interesting to note the broad peak around 6.2 Å on the plot for the O–Hw (solvent water hydrogen) interaction. This could indicate the start of a new solvation shell. The PCF between the nitrogen of the solute and the atoms of the solvent is shown in Fig. 3. The N–Hw is not as pronounced as the previous O–Hw peak. Clearly, the steric crowding by four methyl groups around the nitrogen makes it difficult for the nitrogen to interact with the solvent closely. This is consistent with the components of the solvation free energy. Since the solvation is a complex process, it is hard to directly relate the solvation structure and the spectral shift. The strong hydration on oxygen atom in aqueous solution may cause to stabilize *n* orbital (HDOMO), which is mainly localized on the

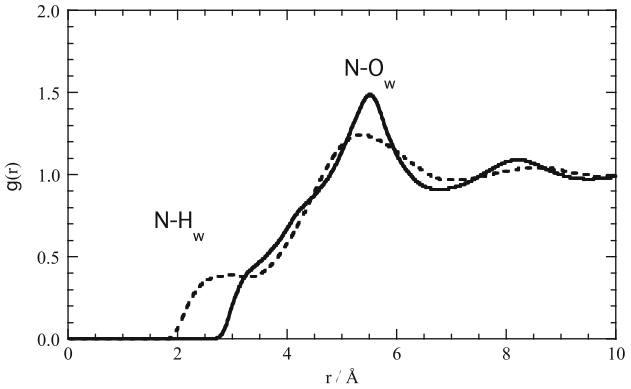

Fig. 3 Pair correlation function between the nitrogen in TEMPO and the solvent water molecules. The *continuous line* represents the solvent oxygen while the *broken line* the solvent hydrogen

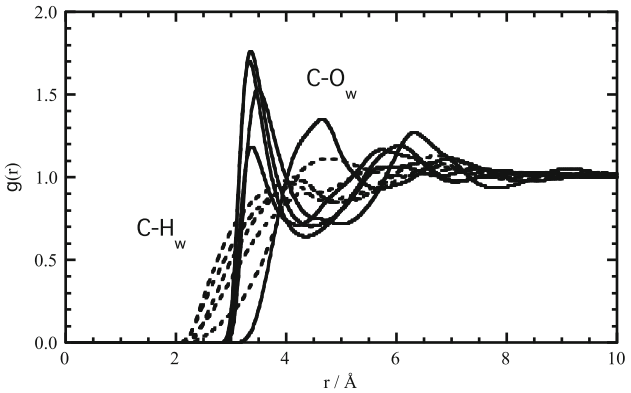

Fig. 4 Pair correlation function between the carbons in TEMPO and the solvent water molecules. The *continuous line* represents the solvent oxygen while the *broken line* the solvent hydrogen

oxygen and to widen the orbital gap between n and π^*. Consequently the blue shift was observed.

The PCF between the carbons of the solute and the atoms of the solvent is shown in Fig. 4. The five different carbon types of TEMPO are visibly distinguished by their PCF. Four of them have similar sharp peak locations, differing only on the height of their peaks, but one has a peak that is visibly shifted away from the other carbons. This shifted peak is the PCF between the solvent oxygen and the solute carbon directly attached to the nitrogen. This is the carbon that has 2 methyl substituents. It is evident that steric considerations also hinder its close interaction with the solvent. Similar observation can be inferred from the PCF between the solvent hydrogen and the solute carbons, although the peaks are relatively less pronounced.

4 Conclusions

We have examined the solvent effect of TEMPO, a well-known stable free radical compound in solution phase. The computed excited energies in various solvent show good agreement with experimental values. The spectra is essentially attributed to the $n \rightarrow \pi^*$ transition corresponding to HDOMO–LUMO transition in β-spin orbitals. The solvent effect on the spectrum is explained as the alteration of the corresponding orbital gap.

Acknowledgments The authors wish to express their thanks to Professor Keiji Morokuma (FIFC, Kyoto University) for giving us the opportunity of collaboration. This work was supported by the Japan-East Asia Network of Exchange for Students and Youths (JENESYS). MJFF wishes to thank MSU-IIT and the Commission on Higher Education (CHED) for the scholarship and support. The work is also financially supported in part by Grant-in-Aid for Scientific Research on Priority Areas "Molecular Science for Supra Functional Systems" (477-22018016), Grant-in-Aid for Scientific Research on Innovative Areas "Molecular Science of Fluctuations" (2006-21107511), as well as by Grant-in-Aid for Scientific Research (C) (20550013).

References

1. Wentrup C (2002) Science 295:1846
2. Matyjaszewski K (1998) In: ACS symposium series, controlled radical polymerization. American Chemical Society
3. Georges MK, Veregin RPN, Kazmaier PM, Hamer GK (1993) Macromolecules 26:2987–2988
4. Debuigne A, Radhakrishnan T, Georges MK (2006) Macromolecules 39:5359–5363
5. Fouassier JP (ed) (2006) Photochemistry and UV curing: new trends. Research Signpost, Trivandrum
6. Mel'nikov MYa, Smirnov VA (1994) Fotokhimiya organischeskikh radikalov (Photochemistry of organic radicals). Mosk. Gos. University, Moscow
7. Keana JFW, Lex L, Mann JS, May JM, Park JH, Pou S, Prabhu VS, Rosen GM, Sweetman BJ, Wu Y (1990) Pure Appl Chem 62:201
8. Hideg K (1990) Pure Appl Chem 62:207
9. Rassat A (1990) Pure Appl Chem 62:223
10. Sosnovsky GJ (1992) Pharm Sci 81:496
11. Barriga S (2001) Synlett 4:563
12. Lebedev OL, Kazarnovskii SN (1960) Zhur Obshch Khim 30:1631–1635
13. Novak I, Harrison LJ, Kovak B, Pratt LM (2004) J Org Chem 69:7628–7634
14. Griller D, Ingold KU (1976) Acc Chem Res 9:13
15. Green S, Fox MA (1995) J Phys Chem 99:14752–14757
16. Bobbitt JM, Flores CL (1988) Heterocycles 27:509
17. Yamaguchi M, Miyazawa T, Takata T, Endo T (1990) Pure Appl Chem 62:217
18. de Nooy AEJ, Besemer AC, van Bekkum H (1996) Synthesis 1153-1174
19. Janowski A, Turowska-Tyrk I, Wrona PK (1985) J Chem Soc Perkin Trans II 821
20. Lalevee J, Allonas X, Jacques P (2006) J Mol Struct (THEOCHEM) 767:143–147
21. Hirata F, Sato H, Ten-no S, Kato S (1998) In: ACS symposium series, combined quantum mechanical and molecular mechanical methods. American Chemical Society
22. Hirata F, Sato H, Ten-no S, Kato S (2001) In: Becker MO, MacKerell DA, Roux B, Watanabe M (eds) Computational biochemistry and biophysics. Marcel Dekker Inc., New York
23. Ten-no S, Hirata F, Kato S (1994) J Chem Phys 100:7443

24. Sato H, Hirata F, Kato S (1996) J Chem Phys 105:1546
25. Yokogawa D, Sato H, Sakaki S (2007) J Chem Phys 126:244504
26. Yokogawa D, Sato H, Sakaki S (2009) J Chem Phys 131:214504
27. Yokogawa D, Sato H, Sakaki S, Kimura Y (2010) J Phys Chem B 114:910–914
28. Schmidt MW, Baldridge KK, Boatz JA, Elbert ST, Gordon MS, Jensen JH, Koseki S, Matsunaga N, Nguyen KA, Su SJ, Windus TL, Dupuis M, Montgomery JA (1993) J Comput Chem 14:1347–1363
29. Becke AD (1988) Phys Rev A 38:3098
30. Perdew JP, Wang Y (1991) Phys Rev B 45:13244
31. Singer SJ, Chandler D (1985) Mol Phys 55:621
32. Jorgensen WL, Briggs JM, Contreras ML (1990) J Phys Chem 94:1683–1686
33. Jorgensen WL (1986) J Phys Chem 90:1276
34. Jorgensen WL, Madura JD, Swenson CJ (1984) J Am Chem Soc 106:6638
35. Jorgensen WL, Briggs JM (1988) Mol Phys 63:547
36. Fox T, Kollman PA (1998) J Phys Chem B 102:8070
37. Capiomont A, Lajzérowicz-Bonneteau J (1974) Acta Cryst B30:2160–2166
38. Kimura K, Katsumata S, Achiba Y, Yamazaki T, Iwata S (1981) Handbook of HeI spectra of fundamental organic molecules. Japan Scientific Societies Press, Tokyo
39. Hirata S, Lee TJ, Head-Gordon M (1999) J Chem Phys 111:8904–8912
40. Iida K, Sato H, Sakaki S (2009) J Chem Phys 130:044107